CellPress

Molecular Cell
Review

Unique Roles of the Non-identical MCM Subunits in DNA Replication Licensing

Yuanliang Zhai,[1,5,*] Ningning Li,[2] Hanlun Jiang,[3] Xuhui Huang,[3] Ning Gao,[2,4,*] and Bik Kwoon Tye[1,6,*]
[1]Division of Life Science, Hong Kong University of Science and Technology, Clear Water Bay, Kowloon, Hong Kong, China
[2]State Key Laboratory of Membrane Biology, Peking-Tsinghua Center for Life Sciences, School of Life Sciences, Peking University, Beijing, China
[3]Department of Chemistry, Hong Kong University of Science and Technology, Clear Water Bay, Kowloon, Hong Kong, China
[4]Ministry of Education Key Laboratory of Protein Sciences, Beijing Advanced Innovation Center for Structural Biology, School of Life Sciences, Tsinghua University, Beijing, China
[5]Institute for Advanced Study, Hong Kong University of Science and Technology, Clear Water Bay, Kowloon, Hong Kong, China
[6]Department of Molecular Biology and Genetics, College of Agriculture and Life Sciences, Cornell University, Ithaca, NY, USA
*Correspondence: zhai@ust.hk (Y.Z.), gaon@pku.edu.cn (N.G.), biktye@ust.hk (B.K.T.)
http://dx.doi.org/10.1016/j.molcel.2017.06.016

A family of six homologous subunits, Mcm2, -3, -4, -5, -6, and -7, each with its own unique features, forms the catalytic core of the eukaryotic replicative helicase. The necessity of six similar but non-identical subunits has been a mystery since its initial discovery. Recent cryo-EM structures of the Mcm2–7 (MCM) double hexamer, its precursors, and the origin recognition complex (ORC)-Cdc6-Cdt1-Mcm2–7 (OCCM) intermediate showed that each of these subunits plays a distinct role in orchestrating the assembly of the pre-replication complex (pre-RC) by ORC-Cdc6 and Cdt1.

The Replicon Model of DNA replication, beginning with the binding of an initiator at a replication origin followed by the recruitment of other replication proteins that unwind and replicate DNA from the origin (Jacob et al., 1964), is shared in all three kingdoms of life. However, the details of how this process is achieved have diverged considerably (reviewed by Bleichert et al., 2017). Briefly, in prokaryotes, DnaA binds multiple motifs at the replication origin and oligomerizes to form a supra-nucleoprotein structure that melts the adjacent AT-rich region to form an initiation bubble (Bramhill and Kornberg, 1988; Duderstadt et al., 2011; Gille and Messer, 1991; Richardson et al., 2016; Speck and Messer, 2001). The DnaB helicase in the form of a hexameric ring is loaded one each on opposite lagging strands by the helicase loader, DnaC (Arias-Palomo et al., 2013).

In eukaryotes, initiation of DNA replication begins with the binding of the origin recognition complex (ORC) and Cdc6 to replication origins. Unlike the prokaryotic initiator that melts origin DNA (Bleichert et al., 2017), in the budding yeast, ORC-Cdc6 only plays the role of origin recognition (Duzdevich et al., 2015; Mizushima et al., 2000; Speck and Stillman, 2007) and a scaffold for assembling the 12-subunit Mcm2–7 double hexamer (DH) (Evrin et al., 2009; Remus et al., 2009), known as the pre-replication complex (pre-RC) that licenses replication origins. Melting of origin DNA appears to be carried out during the transition of the inert Mcm2–7 (MCM) DH to form a pair of bidirectional replicative helicases (Li et al., 2015; Martinez et al., 2017; Parker et al., 2017). The biochemistry and genetics on this subject accumulated throughout the years suggest that this process is much more complicated in eukaryotes, and they have been summarized periodically by in-depth reviews (Bell and Labib, 2016; Costa et al., 2013; Deegan and Diffley, 2016; Samson and Bell, 2013). Putting these disjointed pieces of information together without a structural framework has been difficult. Extrapolating from the simpler models of archaea, which have homologs of Orc1/Cdc6 and Mcm, has been useful (Chong et al., 2000; Samson and Bell, 2016; Slaymaker and Chen, 2012), especially with the early crystal structures of portions of these proteins (Fletcher et al., 2003; Miller and Enemark, 2015). However, the simplified model exactly lacks the intricacies of eukaryotes that have puzzled researchers. High-resolution structures of the eukaryote replication machinery are key to assembling this elaborate puzzle.

Until only very recently, sub-nanometer high-resolution structures of the critical components of the DNA replication initiation molecular assembly were rare (Table 1). With the advent of the resolution revolution of cryoelectron microscopy (cryo-EM), a few of these critical structures became available. In particular, the Mcm2–7 single hexamer (MCM-SH) (7.3 Å) (Zhai et al., 2017), the Cdt1-Mcm2–7 (CM) heptamer (7.1 Å) (Zhai et al., 2017), the ORC-Cdc6-Cdt1-Mcm2–7 (OCCM) intermediate (3.9 Å) (Yuan et al., 2017), and the Mcm2–7 double hexamer (MCM-DH) (3.8 Å) (Li et al., 2015) provide a series of snapshots that show a glimpse of the sequence of events that leads to replication licensing in *Saccharomyces cerevisiae*. This exciting development provides the much-needed structural framework to organize the wealth of genetic and biochemical details that researchers have accumulated. In this review, we try to integrate the many seemingly disjointed pieces of biochemical and genetic information into these snapshots to produce two animated sequels of the assembly process of the MCM-DH. Throughout this exercise, we point out the missing links and speculative hypotheses used to fill the gaps, hopeful and mindful that a fuller and more accurate picture will be forthcoming.

The MCM Family of Six, Each with Unique Features and Specific Roles

The MCM mutants were named after the minichromosome maintenance screen designed to identify replication initiation mutants

Table 1. Structures Related to DNA Replication Licensing

Replication Complex		Source	Size (MDa)	Resolution (Å)	Method	EMD or PDB (Special Feature)	Reference
Origin recognition complex	Orc1-5	yeast	0.36	25	NS-EM (120 kV)	EMD: 5013	Chen et al., 2008
	Orc1-6	fly	0.39	22	NS-EM (120 kV)	EMD: 2479	Bleichert et al., 2013
	trimmed Orc1-6	fly	0.28	3.5	X-ray diffraction	PDB: 4xgc	Bleichert et al., 2015
	trimmed Orc1-5	human	0.28	18	cryo-EM (300 kV)	EMD: 8541; PDB: 5ujm	Tocilj et al., 2017
	trimmed Orc1/4/5	human	0.16	3.39	X-ray diffraction	PDB: 5uj7	Tocilj et al., 2017
	trimmed Orc2/3	human	0.12	6	X-ray diffraction	PDB: 5uj8	Tocilj et al., 2017
ORC-Cdc6-DNA		yeast	0.5	15	cryo-EM (200 kV)	EMD: 5381	Sun et al., 2012
Mcm2–7		fly	0.54	33	NS-EM (120 kV)	EMD: 1834	Costa et al., 2011
		fly	0.54	35	NS-EM (120 kV)	EMD: 1835	Costa et al., 2011
		human	0.567	23	NS-EM (120 kV)	EMD: 2872	Hesketh et al., 2015
		human	0.567	23	NS-EM (120 kV)	EMD: 2873 (DNA bound)	Hesketh et al., 2015
		yeast	0.606	8	cryo-EM (300 kV)	EMD: 6673 (AMPPNP bound)	Zhai et al., 2017
		yeast	0.606	7.3	cryo-EM (300 kV)	EMD: 6674 (ADP bound)	Zhai et al., 2017
Cdt1-Mcm2–7		yeast	0.675	7.1	cryo-EM (300 kV)	EMD: 6671 (AMPPNP bound); PDB: 5h7i	Zhai et al., 2017
		yeast	0.675	7.1	cryo-EM (300 kV)	EMD: 6672 (ADP bound)	Zhai et al., 2017
ORC-Cdc6-Cdt1-Mcm2–7 (OCCM)		yeast	1.1	14	cryo-EM (200 kV)	EMD: 5625	Sun et al., 2013
		yeast	1.1	3.9	cryo-EM (300 kV)	EMD: 8540; PDB: 5udb	Yuan et al., 2017
Mcm2–7 double hexamer		yeast	1.2	30	NS-EM (120 kV)	data not deposited	Remus et al., 2009
		yeast	1.2	15	cryo-EM (200 kV)	EMD: 5857	Sun et al., 2014
		yeast	1.2	3.8	cryo-EM (300 kV)	EMD: 6338; PDB: 3ja8	Li et al., 2015

in yeast (Gibson et al., 1990; Maine et al., 1984). Although multiple homologs of the MCM proteins or mutants were identified in different organisms often based on phenotypes unrelated to DNA replication functions (Holthoff et al., 1996; Kubota et al., 1997; Moir et al., 1982), only six of them were ubiquitous to all eukaryotes from yeast to human. They were named Mcm2, Mcm3, Mcm4, Mcm5, Mcm6, and Mcm7. Despite their similarity, early yeast studies showed that each was indispensable for growth (Yan et al., 1991) and for DNA replication (Labib et al., 2000). Since a single homolog identified in the archaea can form a hexameric ring helicase, an immediate curiosity was why eukaryotes need six homologous subunits to form a heterohexameric ring helicase.

A sequence and structural comparison of the six eukaryotic MCM homologs with the archaeal homolog shows that the core that defines the structural NTD (N-terminal domain) and CTD (C-terminal domain) as well as the catalytic function of the MCM helicase is highly conserved (Figure 1A; Figure S1). Both the archaeal and the eukaryotic MCMs also contain CTEs (C-terminal extensions) (magenta), but these domains appear to be highly divergent both in sequence and in length (Figure 1A; Figure S1). Features absent from the archaeal MCM are the NTEs (N-terminal extensions) (lime green), NTIs (N-terminal insertions), N-C linker insertions, and CTIs (C-terminal insertions) (red) (Figure 1A). All of these elements are unique in sequence among members of the MCM family but mostly conserved with some exceptions among individual homologs across species (Figure S1), suggesting that they play conserved and specific roles.

Defined Roles of the Individual CTEs of the Mcm2–7 Hexamer during Loading

Four MCM-related cryo-EM structures, Mcm2–7, CM, OCCM, and the DH that became available recently provide a trove of information of how the MCM-DH is assembled by ORC-Cdc6. In particular, since Cdt1-MCM is the precursor of OCCM and OCCM is the precursor of MCM-DH, these structures inform how the unique elements of each of the MCMs behave during the assembly process. Figure 2 illustrates the precursor-product relationship of these transitional structures in different views, starting from top to bottom. If we first focus on the CTEs, in the CM heptamer (Figures 1B and 2E–2H), which is a left-handed open coil with a narrow gate of 10–15 Å, only the CTEs of Mcm2, Mcm4, Mcm5, and Mcm6 are structured (Figure 1B, in magenta). The Mcm5-CTE deposits its wing helix domain (WHD) in the central channel (Figures 2A, 2B, 2E, 2F, and 3E–3G), while the CTEs of Mcm4 and Mcm6 form a pseudo-dimer above the core of the coil (Figures 2B, 2D, 2F, and 2H). The narrow gate and the spatial arrangement of the CTEs of Mcm4 and Mcm5 largely block the entry of duplex DNA into the MCM coil (Figures 2E, 2F, and 3E–3G). Consistent with these structural features, biochemical studies show that the CM heptamer cannot be loaded onto double-stranded DNA (dsDNA) spontaneously (Bochman and Schwacha, 2007; Bowers et al., 2004; Coster et al., 2014; Evrin et al., 2009; Frigola et al., 2013; Heller et al., 2011; Kang et al., 2014; Remus et al., 2009).

In the OCCM, the previously non-discernible Mcm3-CTE becomes visible as a wing helix at the very end, extending well above the MCM CTD ring through a long flexible linker to lodge

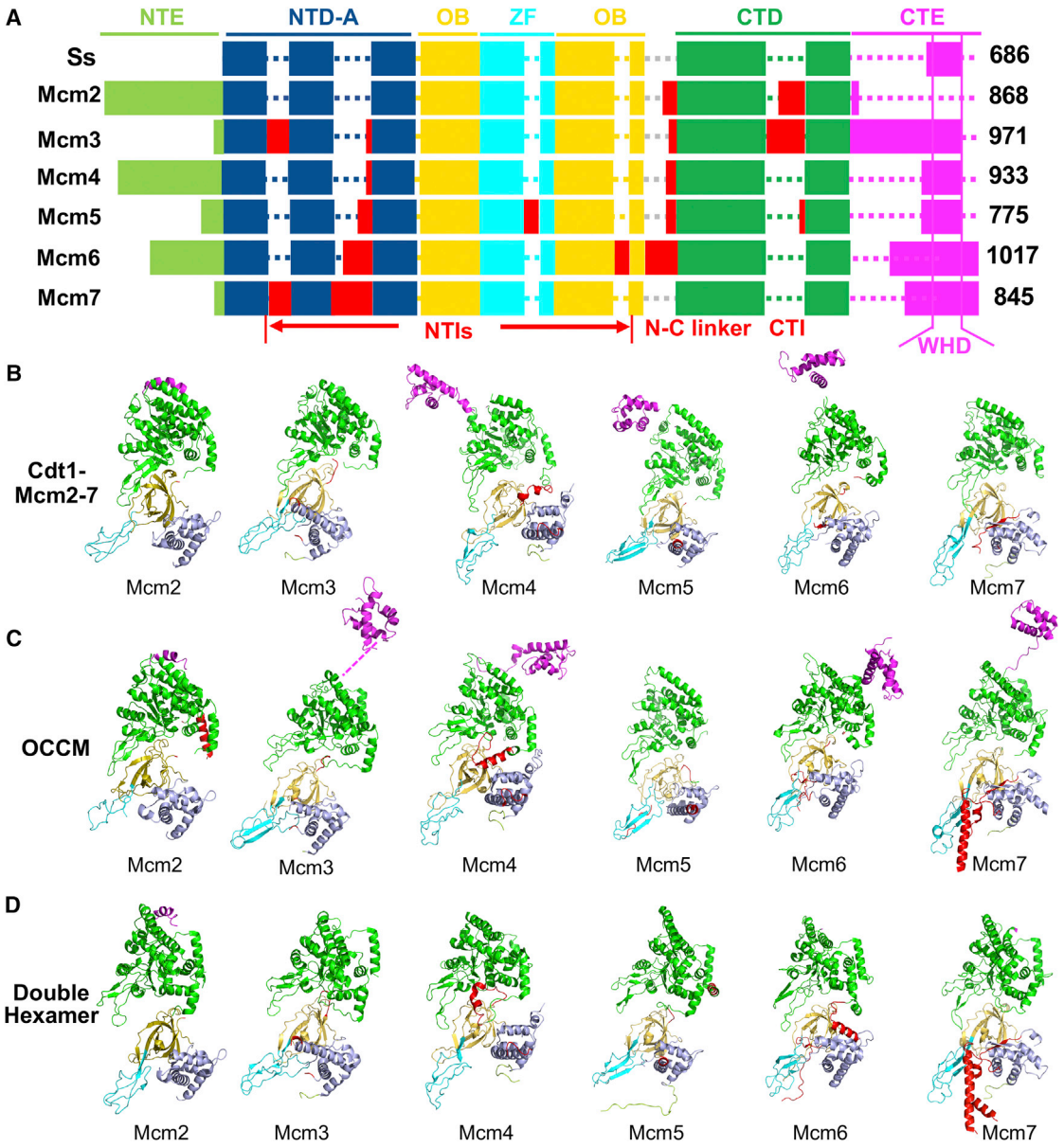

Figure 1. Subunit-Specific Structural Features of the Mcm2–7 Subunits

(A) Schematic illustration of domain organization and subunit-specific features of the *S. cerevisiae* Mcm2–7 subunits compared to the archaeal MCM (*Ss*, *Sulfolobus solfatoricus*). NTE, N-terminal extension; NTD-A, N-terminal domain A; OB, oligonucleotide-binding fold; ZF, zinc finger; CTD, C-terminal domain; CTE, C-terminal extension; NTI, NTD insertion; N-C linker, NTD CTD linker; CTI, CTD insertion; WH, wing helix.

(B–D) Side-by-side structural comparison of Mcm2–7 subunits from CM (PDB: 5h7i) (B), OCCM (PDB: 5udb) (C), and Mcm2–7 DH (PDB: 3ja8) (D) using the OB domain as a reference for alignment. Not shown are subunit structures of Mcm2–7 single hexamer because of their similarity to CM.

its C-terminal wing helix domain (cWHD) onto the surface created by Cdc6-Orc2 (Figures 1B, 1C, 2A–2L, 3A, and 3C). The role of Mcm3-cWHD in the docking of the MCM onto ORC-Cdc6 has been well documented (Frigola et al., 2013). Previous study showed that truncation and mutations of the cWHD of Mcm3 block the loading of MCM onto ORC-Cdc6, precluding any interaction between ORC-Cdc6 (OC) and MCM. This result suggests that Mcm3-cWHD makes the first necessary contact between OC and MCM. Moreover, the Mcm3-CTE fragment alone can bind OC and activate its ATPase (Fernández-Cid et al., 2013; Frigola et al., 2013), which presumably triggers a series of allosteric conformational changes of the OC to engage with other MCM subunits. It is noteworthy that OCCM can be formed in the presence of ATP-γ-S, suggesting that, up to this point, assembly of this intermediate complex is largely independent of ATP hydrolysis by OC or Mcm2–7 (Fernández-Cid et al., 2013; Frigola et al., 2013; Sun et al., 2013; Yuan et al., 2017).

Subsequent anchoring of the MCM to OC facilitated by the rearrangements of the cWHDs of other MCM subunits is evident by the structural comparison between CM and OCCM (Figures 3A,

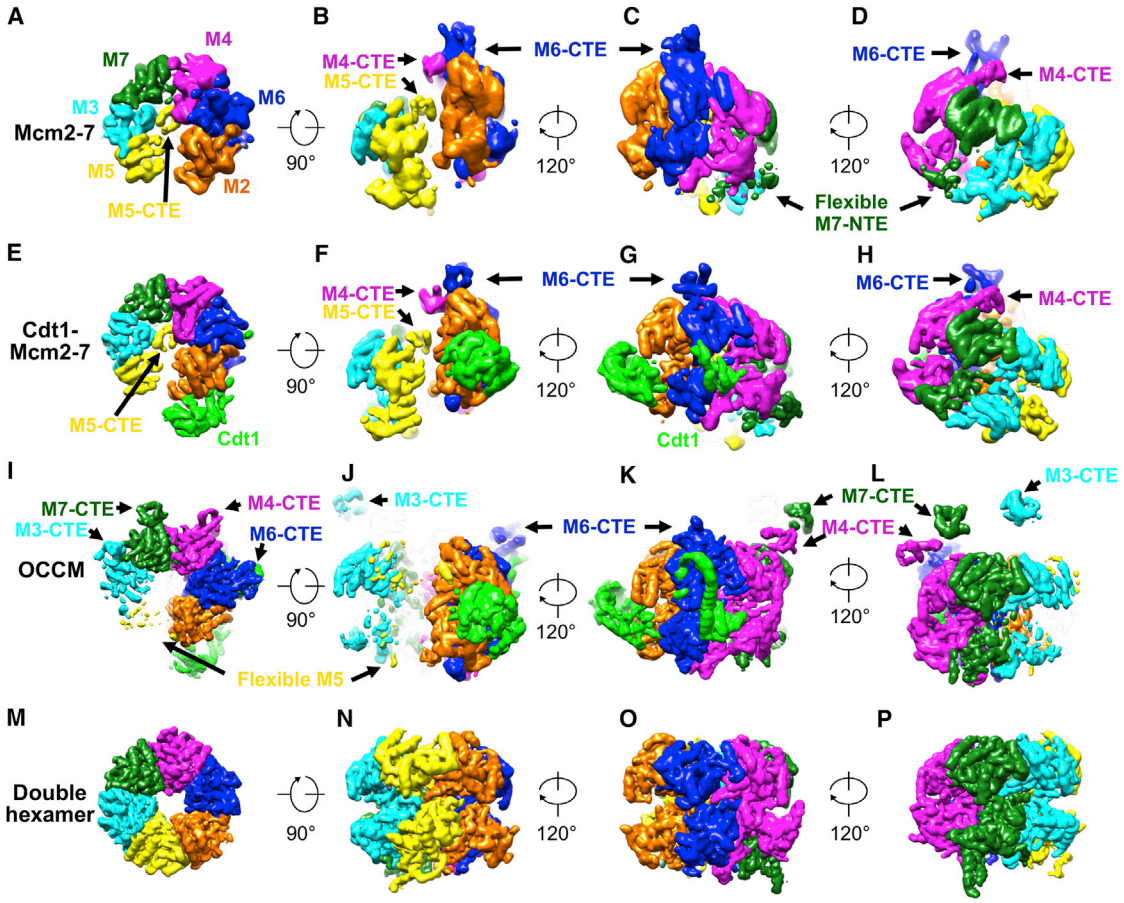

Figure 2. Comparison of the Overall Structures of the Mcm2–7 Complexes Related to Replication Licensing

(A–P) Cryo-EM maps, shown in surface representation, of the Mcm2–7 single hexamer (EMD: 6674) (A–D), the Cdt1-MCM heptamer (EMD: 6671) (E–H), OCCM (EMD: 8540, only Cdt1-Mcm2-7 is shown) (I–L), and Mcm2–7 DH (EMD: 6338, only half of DH is shown) (M–P). Subunits are color coded as indicated by the labels. Top (A, E, I, and M) and side views (all other panels) are shown. Visual effect with depth cueing was applied such that Mcm7 in the back side is hardly visible in (B), (F), and (J).

3E, and 3F). The previously non-discernible Mcm7-CTE (Figures 1B, 2D, and 2H) is also visible as a structured WHD (Figures 1C, 2K, and 2L), and it binds to the surface created by Orc1-Cdc6 (Figure 3C). It is likely that the anchoring of Mcm4-cWHD and Mcm6-cWHD (Figure 3A) that follows orients the MCM coil such that the Mcm2-Mcm5 gate is aligned with the duplex DNA encircled by OC (Figure 3B). Interestingly, in the OCCM structure (EMD: 8540), the electron density of the entire Mcm5 is highly reduced compared to other subunits (Figures 2I and 2J), suggesting that Mcm5 is flexibly linked to Mcm3 or Mcm5 adopts alternative conformations at this stage. Perhaps, this flexibility or conformational change in Mcm5 helps duplex DNA to pass through the narrow Mcm2-Mcm5 gate. We believe that the interactions between the MCM-cWHDs and OC as well as the interactions between the central channel and DNA induce a conformational change of the Cdt1-MCM heptamer from coil to near planar. During the transition, a number of conformational changes involving the MCM CTEs must take place. Mcm5-cWHD must vacate the MCM central channel (Figures 3E–3G). The Mcm4-cWHD and Mcm6-cWHD must rearrange their positions to clear the steric hindrance that prevents the docking of MCM onto OC and dsDNA (Figures 3E and 3F). In football speak, the CTEs of the MCM must rearrange from a defensive formation that prevents premature loading in the Cdt1-MCM to an offensive formation that anchors the MCM onto OC in the OCCM.

So far, it is unclear whether these CTEs play a role in loading the second CM, with the exception of the Mcm3-CTE (Frigola et al., 2013). However, once the loading process is complete and a stable MCM-DH is formed, all CTEs of the MCM subunits become flexible to the extent that their structures are no longer discernible by cryo-EM (Figures 1D and 2M–2P) (Li et al., 2015). Indeed, we cannot distinguish between mobile motifs and unstructured motifs when they are not discernible by cryo-EM. Throughout this review, we use the terms unstructured, flexible, and disorder loosely for lack of information.

The Role of Cdt1 in the Assembly of the MCM-DH

The structure of the full-length Cdt1 has been difficult to determine because of its flexibility. However, its structure in complex with Mcm2–7 and as a component of OCCM was recently determined to contain three domains, NTD, MD (middle domain), and CTD with MD and CTD connected by the flexible M-C linker (Figure 4A). In complex with Mcm2–7, Cdt1 acts as a chaperone

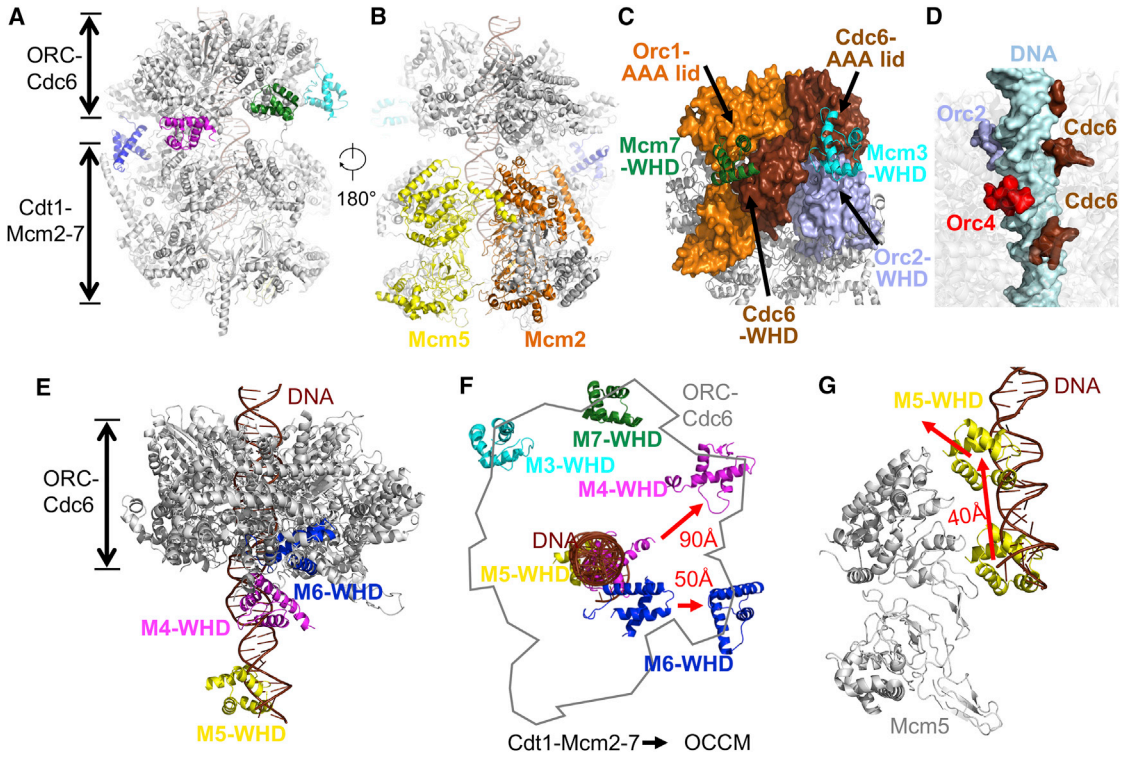

Figure 3. Rearrangements of the MCM CTEs during MCM Loading

(A and B) Front and back views of the OCCM structure (PDB: 5udb). Highlighted in colors are CTEs in (A) and the gate-forming subunits Mcm2 and Mcm5 in (B).

(C) Contact surfaces created by ORC and Cdc6 for WHDs of M3 and M7.

(D) Cdc6 and DNA contact points in OC.

(E–G) Steric hindrance for MCM loading imposed by the CTEs from Mcm4, Mcm5, and Mcm6 of the Cdt1-MCM heptamer (PDB: 5h7i). The structures of the Cdt1-MCM and the OCCM were superimposed by aligning the Mcm2-CTD. (E) Side view shows the superimposed structures of OC-DNA (in gray) derived from OCCM and the cWHDs (color coded) from Cdt1-MCM heptamer. (F) Top view shows the aligned structures in (E). Outline traces the contour of OC. During the transition from Cdt1-Mcm to OCCM, the cWHDs of Mcm4, 5, and 6 undergo translocation as indicated by arrows, while the CTEs of Mcm3 and 7 form structured cWHD. (G) The putative pathway of Mcm5-cWHD translocation in transitioning from Cdt1-MCM to OCCM is shown. The lower position indicates the initial location of Mcm5-WHD in the Cdt1-MCM using Mcm2-CTD as reference for alignment with OCCM; the upper position is its intermediate location using Mcm5-CTD as reference for alignment. Further translation of the Mcm5-WHD is suggested as the arrow-headed direction.

by interacting with the NTDs of Mcm2, Mcm6, and Mcm4 to stabilize the overall structure of the left-handed open coil (Figures 2C, 2D, and 2F–2H) (Zhai et al., 2017). As a component of the OCCM, Cdt1 readjusts its CTD to interact with Mcm6-cWHD (Figures 2K and 4) (Yuan et al., 2017), which may contribute to the latching of the Mcm6-cWHD onto OC (Figures 3A and 3F) and conversion of the coil-to-ring structure of the Mcm2–7. There are ample biochemical and structural data to support this notion.

Previous biochemical data showed that the Mcm6-CTE has an auto-inhibitory function that prevents MCM interaction with OC in the absence of Cdt1 (Fernández-Cid et al., 2013). The CTD of Cdt1 appears to be able to counteract this auto-inhibitory effect of the Mcm6-CTE. Nuclear magnetic resonance (NMR) spectroscopy analysis showed that $Mcm6^{908–970}$ interacts with $Cdt1^{481–501}$ (Liu et al., 2012), as predicted in yeast two-hybrid analyses (Yanagi et al., 2002; Zhang et al., 2010). A conformational change in the $Cdt1^{481–501}$ region from an unstructured to a structured configuration is clearly observable in the cryo-EM structures of Cdt1-MCM and OCCM (Figures 2 and 4). In vitro studies showed that loading of MCM without Cdt1 results in an unstable OC-MCM that readily loses Mcm2, Mcm6, and Mcm4 but retains Mcm5, Mcm3, and Mcm7 (Frigola et al., 2013), with much reduction in the OC-MCM interaction. This result suggests that, in the absence of Cdt1, the MCM ring is prone to breaking into two halves between Mcm7 and Mcm4. This break junction is consistent with the cWHDs of Mcm3 and Mcm7 in contact with OC, while the cWHDs of Mcm6 and Mcm4 are unable to latch onto OC without Cdt1. Cdt1 probably plays an important role in facilitating the latching of cWHDs of Mcm6 and Mcm4 onto OC to effect conformational changes.

Several studies indicate that Cdt1 interacts with Orc6 as well (Asano et al., 2007; Chen et al., 2007; Heller et al., 2011; Wu et al., 2012). This interaction can be detected in the OCCM by cross-linking mass spectrometry (Yuan et al., 2017). Unfortunately, because of the instability of Orc6 in the high-resolution OCCM structure, this interaction was not resolved by cryo-EM.

Animation of the Loading of Cdt1-MCM onto OC Scripted from Biochemical, Genetic, and Structural Data

Cdc6 and Cdt1 play critical roles in orchestrating the docking of MCM onto OC. Cdc6 joins ORC to encircle duplex origin DNA by

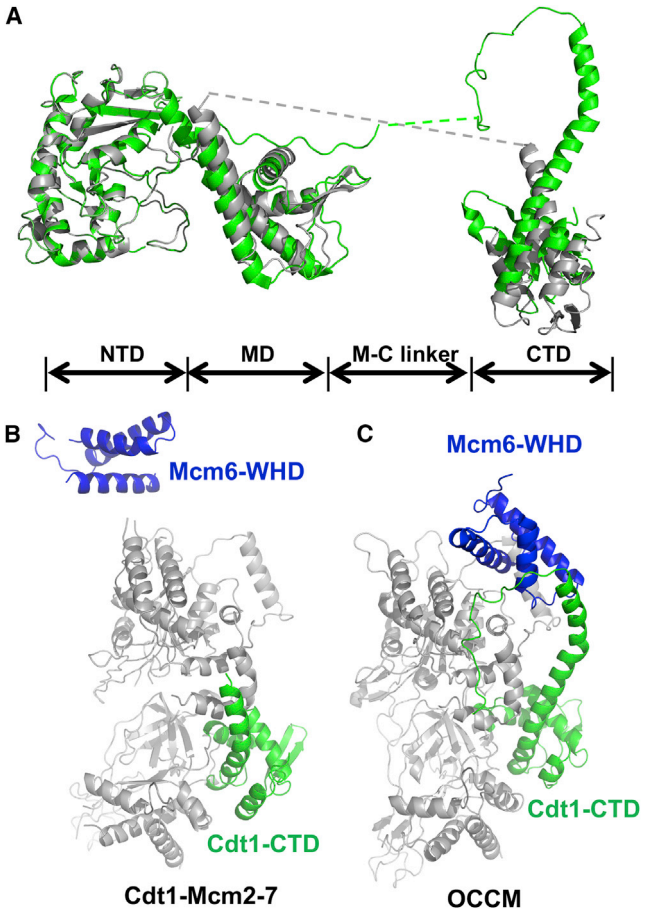

Figure 4. The Conformational Changes of Cdt1-CTD and Mcm6-cWHD during OCCM Formation

(A) Superimposition of Cdt1 in Cdt1-MCM (gray) (PDB: 5h7i) and in OCCM (green) (PDB: 5udb) in schematically organized domains.

(B and C) The relative positions of Cdt1-CTD (green) with Mcm6-WHD (blue) in Cdt1-MCM (B) and OCCM (C).

contacting DNA at three points (Figure 3D) and to create binding surfaces for the anchoring of the cWHDs from Mcm3 and Mcm7 (Figure 3C). Cdt1 stabilizes the MCM-SH for loading. Interactions among OC, MCM, and DNA induce the conformational change that transforms MCM from coil to near planar ring. This transition requires the direct interaction between Cdt1-CTD and the Mcm6-CTE to relieve the inhibitory effect imposed by Mcm6 upon MCM loading.

The dynamic motions of the searching, anchoring, loading, and docking of CM to OC implicated by the structural changes observed between CM and OCCM, and especially changes between floppy and structured components, are best illustrated by animation (Movie S1). One cannot overemphasize the important roles played by the flexible domains that cannot be captured by image reconstruction through cryo-EM. The flexible MCM-cWHDs and the flexible linker of Cdt1 that connects its MD and CTD likely play a major role in coaxing the coil-to-ring transition of the MCM-SH. The flexible Mcm5 in the OCCM structure (Figures 2I and 2J) suggests that duplex DNA may be able to snug through the narrow gate of the near planar but still open MCM ring. Indeed, in the single-molecule fluorescence resonance energy transfer (FRET) analysis, the change in signal after the release of Cdc6 and Cdt1 from OCCM could reflect the closing of the Mcm2-Mcm5 gate or the transition of the Mcm5 from a flexible to a fixed configuration or both (Ticau et al., 2017). In fact, these changes may coincide with the transition of the coil-to-ring structure, as illustrated by the morphing of the open coil heptamer to a planar ring (Movie S1).

We caution that the animation is generated by the morphing of one complex into the next without knowledge of the intermediary path. The actual MCM-loading mechanism may not be as simple as presented here.

A Speculative Model for the Loading of the Second CM Unit onto ORC-MCM

One of the most intriguing results of the single-molecule FRET studies is the manner in which the MCM-DH is formed (Ticau et al., 2015). The MCM-DH is formed by the loading of two CM heptamers one at a time, with the removal of Cdc6 from ORC and Cdt1 from the MCM hexamer at each interval and the replenishing of Cdc6 between loadings (Sun et al., 2014; Ticau et al., 2017). Importantly, current evidence favors that only one ORC molecule arbitrates the process of two rounds of MCM loading to form a stable MCM-DH. Moreover, we learned from the structures of the MCM hexamer and the CM heptamer that the role of Cdt1 is to stabilize the coil structure, especially the Mcm7-NTD, by interacting with Mcm2, Mcm4, and Mcm6 through allosteric effect (Figures 2D and 2H). We also learned from the near planar ring structure of OCCM that Mcm5 is largely flexible (Yuan et al., 2017) (EMD: 8540). Interestingly, a prominent feature of the MCM-DH is the tight junction between the two head-to-head MCM rings joined inextricably by the NTI and zinc finger (ZF) of Mcm7 and a long NTE of Mcm5 (Li et al., 2015). Both Mcm5-NTE and Mcm7-NTI are flexible in the single hexamer and are stabilized in the DH through direct interactions between them. In this section, we use these pieces of information to weave a sequence of events for the loading of the second Cdt1-MCM in an animation (Movie S2).

Three events must take place before the loading of the second copy of the CM. First, Cdc6 is released in an ATP-dependent manner (Fernández-Cid et al., 2013; Ticau et al., 2017). Release of Cdc6 from ORC would mean the removal of contact surfaces for Mcm3 and Mcm7 from OC (Figure 3C), leaving MCM hanging onto ORC by the CTEs of Mcm4 and Mcm6 (Figure 3A). Second, release of Cdt1 would mean that the Mcm7 NTD also becomes destabilized. Third, the reloading of Cdc6 would keep OC securely bound to DNA (Figure 3D) and recreate the attachment site for the CTE of Mcm3 of the incoming Cdt1-MCM. Based on the OCCM structure, we imagine that the binding of the second Mcm3-CTE to OC may also confer flexibility to the Mcm5 of the second heptamer, which could create a more far-reaching scope for the extended Mcm5-NTE to connect with the Mcm7-NTD of the docked MCM. We envision that when the second CM searches for a launching site, the long flexible Mcm5-NTE of the docked MCM may also reach out for the motifs of the Mcm7-NTD of the incoming heptamer (Figure 1). Once connected, release of Cdc6 would disengage the second CM from OC. A simple flip over the hinges provided by interactions

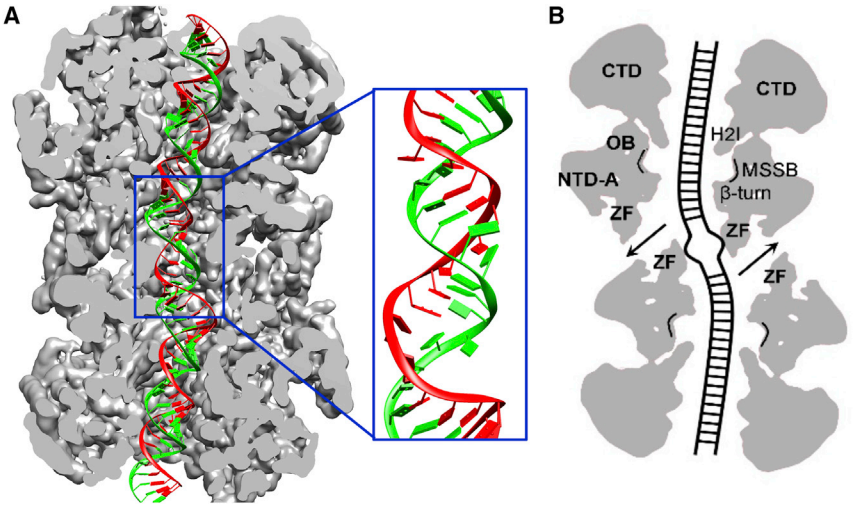

Figure 5. Modeling of MCM-DH DNA Complex

(A) Cut-away view of the density map of the MCM-DH with a piece of origin DNA ARS305 modeled in the central channel. The base pairings of the nucleotides were adjusted according to the spatial restriction of the MCM central channel. The origin DNA embedded in the region of the hexamer interface is shown in magnified view.

(B) Model for initial origin DNA melting, adapted from Li et al. (2015).

The MCM-DH structure refined with NCS restraints was used to model the MCM-DH-DNA complex. Double-stranded DNA (dsDNA) structures with the sequence of the MCM-binding site at ARS305 were inserted into the central channel of each MCM hexamer. Specifically, the dsDNA in each hexamer was rotated along its longitudinal axis to minimize the protein-DNA steric clashes with PyMOL (http://www.pymol.org). Due to the kink at the interface between the two hexamers, fully base-paired dsDNA cannot be accommodated at this region. Therefore, the dsDNA structure at the interface was remodeled by ModeRNA (Rother et al., 2011) and inserted into the central channel. Finally, A 5,000-step energy minimization by ENCAD (Levitt, 1983; Levitt et al., 1995) was performed to further refine the complex structure by eliminating the remaining clashes.

between the two pairs of Mcm5 and Mcm7 would position the Mcm2-Mcm5 gate of the second heptamer along the duplex DNA for loading. Additional interactions between the NTDs of Mcm5 and Mcm7 as well as other Mcm subunits would likely further engage the two hexamers, providing the impetus for the second Cdt1-MCM to dock onto dsDNA. Through an ATP-dependent process, we imagine that, as Cdt1 is released, the incoming MCM would transition from coil to ring, secured by interactions of the zinc finger rings of the two MCMs, leaving behind a rigid, twisted, slightly offset DH. At this point, the contact between the MCM-DH and ORC is no longer secured and the function of ORC is complete.

A cross-section of the structure of the MCM-DH shows that the central channel of the two stacked hexameric rings forms a kink at the interface such that the intervening DNA cannot be accommodated as the Watson-Crick B-form DNA (Figure 5A). In a structural model where dsDNA was computationally built and refined in the central channel, the pairing of as many as seven base pairs has to be disrupted in the twisted, misaligned space (Figure 5A; unpublished data). We believe that these disrupted base pairs may be the nucleation center for DNA melting during the activation of DNA replication initiation (Figure 5B) (Bochman and Schwacha, 2015; Li et al., 2015).

Conservation of the CTEs and Other Unique Features of Individual MCM Subunits across Species

Based on the cross-species sequence homology alignment of each member of the MCM family (Figure S1), it is possible to predict whether each of the unique elements with specific functions in the loading mechanism in yeast is preserved in all eukaryotes, including humans.

An overview of the alignment of sequences between each of the eukaryotic MCM subunits and the *Sulfolobus solfataricus* MCM shows that regions not found in the archaeal MCM tend to be flexible in the eukaryotic MCM, whether in the Cdt1-MCM, OCCM, or DH (Figure S1, tan box). These flexible hinges presumably increase the adaptability and versatility of the entire protein, so that the protein can fold into different conformations as demanded. A closer inspection of these flexible regions in each of the subunits shows that most of them are conserved in both sequence and structure, suggesting a conserved function. These observations speak to the instructive value of flexible domains in dynamic molecules.

The cWHDs of Mcm3, Mcm7, Mcm6, and Mcm4 have been shown to act temporally in the docking of Cdt1-MCM onto OC, and, therefore, they deserve special attention. Sequence alignment shows that all of these cWHD are conserved. Mcm3 has an exceptionally long CTE that is well conserved in the C-terminal 80–90 residues, which fold into the cWHD. Biochemical data in yeast suggest that this cWHD$^{875–971}$ of Mcm3 is essential for the first contact with OC and responsible for triggering the ATPase activity of OC to ensure quality control of OCCM assembly and Cdc6 recycling. The Mcm5-cWHD, which plays an important role in blocking the loading of DNA in the Cdt1-MCM heptamer, is also conserved in all eukaryotes. It is worth noting that, unlike other eukaryotes, the yeast Mcm2 protein of both *S. cerevisiae* and *S. pombe* lacks a CTE that encodes a cWHD.

Finally, the Mcm5-NTE and the MCM7-NTI, which we speculated to provide anchoring in the loading of the second Cdt1-MCM heptamer, are also conserved. However, there is an extra insertion in the *S. cerevisiae* Mcm7-NTI that provides additional contact with the NTD-A of Mcm5 in the DH. NTIs are absent in the archaeal MCM, consistent with biochemical observations that the archaeal MCM-DH can form in solution through zinc finger interactions alone (Chong et al., 2000; Fletcher et al., 2005).

Model of the Two Rounds of MCM Loading for Replication Licensing

A number of models have been proposed to explain the biochemical data for the assembly of the pre-RC (Riera et al., 2014; Samson and Bell, 2013; Yardimci and Walter, 2014).

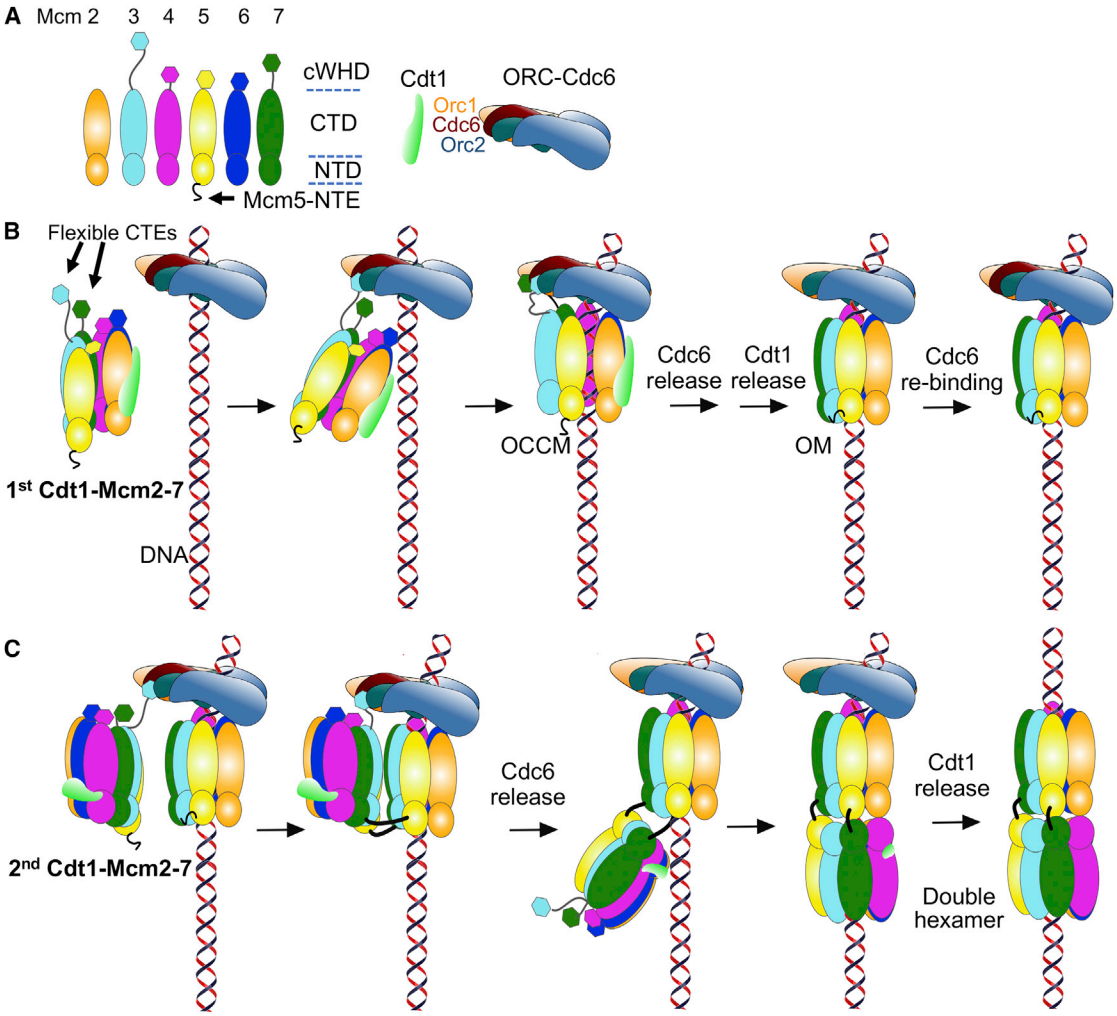

Figure 6. The Acrobat Model for the Independent Loading of the Two MCM Heptamers by a Single ORC
(A) Cartoon representations of structural features of Mcm2–7 subunits, OC and Cdt1.
(B) Loading of the first MCM heptamer by direct anchoring of Mcm3cWHD to OC, followed by Mcm7-cWHD, Mcm6-cWHD, and Mcm4-cWHD, to form OCCM. Flexible CTEs refer to the unresolved CTE structures presumably due to the flexible linkers to the cWHDs.
(C) Recruitment of the second MCM heptamer by the reciprocal interactions of the flexible Mcm5-NTEs and the Mcm7-NTDs from head-to-head MCM rings.

Each of these models explains some of the data but none of them explains all of the data. Key facts that must be satisfied in a credible model for the assembly of the pre-RC are as follows. First, a single ORC is responsible for the loading of two Cdt1-MCMs. Second, the two Cdt1-MCMs are loaded sequentially one at a time to form a DH in a head-to-head orientation. Third, the two loading events are mechanistically identical, each requiring the presence of Mcm3-CTE, a freshly recruited Cdc6 by ORC, and then the sequential removal of Cdc6 and Cdt1. Since it is well established that Mcm3-CTE interacts with OC in the first loading, it is inferred that the same occurs in the second loading.

Here we have constructed a model of the dynamic process of replication licensing based on existing biochemical data and supported by new information derived from the cryo-EM structures of the CM heptamer, the OCCM, and the MCM-DH (Figure 6). In the loading of the first open-coiled heptamer (Figure 6B), the flexible Mcm3-cWHD in a searching mode lodges onto the surface created by the DNA-bound OC. The launching of the cWHDs of Mcm7, Mcm4, and Mcm6 then follows. The latching of the extra short Mcm4-CTE may impose steric constraint to the OC-CM junction, resulting in the bending of DNA at the interface (Yuan et al., 2017). The attachment of the four cWHDs onto OC positions the heptamer such that the open M2-M5 gate is facing the duplex DNA. Although the M2-M5 gate in the free heptamer coil is too narrow for the passage of duplex DNA, the interaction of the Mcm3-CTE with OC may trigger conformational changes by widening the gate to allow the entry of DNA. The alignment of the positively charged central channel with the negatively charged DNA may aid in this process. The coil-to-ring transition of Mcm2–7 may also take place during this ATP-independent process. Hydrolysis of ATP by OC releases the first Cdc6, followed by Cdt1 release as a result of ATP hydrolysis by MCM (Ticau et al., 2017). The release of Cdc6 destroys the binding surfaces for the cWHDs of Mcm3

and Mcm7, but it leaves the binding surfaces for the cWHDs of Mcm6 and Mcm4 intact in the ORC-Mcm2–7 (OM). This entire process happens within 30 s in vitro.

The loading of the second heptamer (Figure 6C) takes a longer time and requires the replenishment of a fresh Cdc6, which creates a new binding surface for the Mcm3-CTE of the incoming heptamer. Hanging by the Mcm3-CTE, the incoming heptamer is placed juxtaposed to the docked Mcm2–7 ring, which is clasping to ORC by the Mcm6-CTE and Mcm4-CTE, such that the Mcm3 subunits of the two MCMs are face to face. The docked Mcm2–7 ring then recruits the second heptamer via the reciprocal interactions of the NTD of Mcm7 and the NTE of Mcm5 on either side of Mcm3 of the stationed and incoming Mcm2–7 complexes. Upon release of the second Cdc6, the incoming MCM lets go of the Mcm3-CTE attachment while joining hands with the docked MCM at the NTD end. Like an acrobat on a trapeze, the second Cdt1-MCM flips and then grabs hold of the duplex DNA by the M2-M5 gate. The zinc finger rings of the two MCM complexes and the attraction of the positively charged central channel and the negatively charged DNA may coax the incoming heptamer into place. This slow assembly process is complete with the removal of Cdt1 and the fusion of the two head-to-head MCM NTD rings. During this part of the process, ATPase activity of MCM subunits is required. For easy reference, we coined our new model ''the Acrobat Model.''

There are a few important features of the Acrobat Model that are not accounted for in other alternative models. First, there is symmetry in the sequential loading mechanism. Second, the role of Cdc6 in forming a binding surface for the CTE of Mcm3 explains the need for a new round of Cdc6 to engage and disengage the Mcm3-CTE/OC linkage in each round. Third, Mcm3 is the only subunit that forms a head-to-head dimer in the MCM-DH. The acrobatic act in the loading of the second heptamer specifically places the two Mcm3 subunits in that position. Finally, the Mcm5-NTE and Mcm7-NTD play a direct role in recruiting the second MCM complex. Although this model satisfies all of the criteria listed above, there may be alternative models that also satisfy all of the above criteria and additional criteria that we missed. Here we assume that ATP hydrolysis by the second Cdc6 is fast and Cdc6 is released soon after the recruitment of the second heptamer but before its docking. If Cdc6 were to leave after the docking, then the Mcm3-CTE would still be attached and it would be sterically impossible for the second MCM to flip. The Acrobat Model should only be viewed as a working model.

Questions Unanswered

In assembling the latest structural, biochemical, and genetic data into a coherent picture of the replication-licensing mechanism, a set of remaining questions comes into focus. First and foremost, it should be noted that the extent of DNA bound by ORC/Cdc6 in the OCCM structure (Yuan et al., 2017) accounts for less than half of the DNA protected by either ORC (Bell and Stillman, 1992; Rowley et al., 1995) or ORC/Cdc6 (Speck et al., 2005) from DNaseI cleavage. It is possible that the missing Orc6 in the current OCCM structure may explain some of this discrepancy. Another possible explanation is that there is a major recofiguration in the OC complex during the formation of OCCM that reduces the footprint of OCCM on DNA. Although there are a number of reports on the structures of ORC, we still do not have the full picture of how ORC interacts with DNA alone or together with Cdc6 before MCM loading. The current ORC structures either do not contain DNA or are trimmed of flexible but important parts (Bleichert et al., 2015; Tocilj et al., 2017). Until we know how the first Cdc6 alters the structure of ORC, we cannot adequately address how the second Cdc6 functions. More intermediate structures through manipulations of *in vitro* assembly may address some of these questions.

It is still unclear how the docked MCM serves as the scaffold for the recruitment of the second MCM. We hypothesize that the flexibility of the NTDs of the two MCM hexamers provides a trapping mechanism during this process. The bonding between the NTDs and NTEs of reciprocal Mcm7 and Mcm5 subunits of each of the MCM hexamers may be the initiating step. Mutational analysis of the NTI of Mcm7 and NTE of Mcm5 may test some of these predictions. Previous biochemical data showed that the ATPase activities of the Mcm2–7 complex also play important roles in the staged MCM-loading process. However, it is poorly understood how ATP binding and hydrolysis by the Mcm subunits transforms the conformation of the MCM complex for its own loading. Using the well-characterized *mcm* ATPase mutants, it may be possible to capture some of the intermediate assemblies for structural analyses by cryo-EM.

To date, only the structures of the NTEs of Mcm3 and Mcm5 have been determined in the DH. The NTEs of Mcm2, Mcm4, and Mcm6, which are the known substrates of the Cdc7-Dbf4 kinase (DDK) (Deegan et al., 2016; Lei et al., 1997; Ramer et al., 2013; Sheu et al., 2014), have not been determined in the context of the DH. Determining the structure of these long regulatory NTEs will likely come from intermediate assemblies stabilized by DDK. A high-resolution structure of DDK-MCM-DH will richly inform the activation mechanism of the inert MCM-DH (Bochman and Schwacha, 2010).

There are additional questions about the state of the dsDNA-bound MCM-DH. In vitro and some in vivo studies indicate that the DH can move freely along duplex DNA (Gros et al., 2015; Remus et al., 2009), yet the cryo-EM high-resolution structure suggests that the DNA-bound MCM-DH is a rigid, stable structure that twists DNA by a tight grip in an immobile state.

Although we have only focused on the specific roles of each individual MCM subunit during replication licensing in this review, we believe that they each also play unique roles throughout the DNA replication process from initiation to elongation (Huang et al., 2015; Richet et al., 2015; Wang et al., 2015) to termination (Maric et al., 2014). For example, during replication elongation, a conserved region of Mcm2-NTE appears to act as a histone H3-H4 chaperone in the assembly and disassembly of nucleosomes in the context of a replisome (Foltman et al., 2013; Huang et al., 2015). The structure of this Mcm2 region in human has also been determined in complex with the H3-H4 dimer (Huang et al., 2015). We look forward to an era of rapid advances in our understanding of eukaryotic DNA replication as more high-resolution structures of DNA replication intermediates are resolved and the in vitro reconstitution experiments replicate in vivo conditions (Azmi et al., 2017; Devbhandari et al., 2017; Kurat et al., 2017; Yeeles et al., 2017). We foresee that, as flexible domains playing

important roles are identified in cryo-EM structures, NMR spectroscopy will come in handy for detailing the dynamics of these key flexible domains.

SUPPLEMENTAL INFORMATION

Supplemental Information includes one figure and two movies and can be found with this article online at http://dx.doi.org/10.1016/j.molcel.2017.06.016.

ACKNOWLEDGEMENTS

We thank all of the reviewers for their constructive and invaluable comments. This work was supported by the Research Grants Council of Hong Kong (GRF16138716 to B.K.T.; GRF16104115 and GRF16143016 to Y.Z. and B.K.T.; IGN15SC02 to Y.Z.; and AoE/P-705/16 to X.H.), the Ministry of Science and Technology of China (grants 2013CB910404 and 2016YFA0500700 to N.G.), the National Natural Science Foundation of China (grants 31422016, 31470722 and 31630087 to N.G.), and the China Postdoctoral Science Foundation (2017M610013 to N.L.). N.L. is supported by Young Elite Scientists Sponsorship Program by CAST and a postdoctoral fellowship from the Peking-Tsinghua Center for Life Sciences.

REFERENCES

Arias-Palomo, E., O'Shea, V.L., Hood, I.V., and Berger, J.M. (2013). The bacterial DnaC helicase loader is a DnaB ring breaker. Cell *153*, 438–448.

Asano, T., Makise, M., Takehara, M., and Mizushima, T. (2007). Interaction between ORC and Cdt1p of Saccharomyces cerevisiae. FEMS Yeast Res. *7*, 1256–1262.

Azmi, I.F., Watanabe, S., Maloney, M.F., Kang, S., Belsky, J.A., MacAlpine, D.M., Peterson, C.L., and Bell, S.P. (2017). Nucleosomes influence multiple steps during replication initiation. eLife *6*, e22512.

Bell, S.P., and Labib, K. (2016). Chromosome duplication in Saccharomyces cerevisiae. Genetics *203*, 1027–1067.

Bell, S.P., and Stillman, B. (1992). ATP-dependent recognition of eukaryotic origins of DNA replication by a multiprotein complex. Nature *357*, 128–134.

Bleichert, F., Balasov, M., Chesnokov, I., Nogales, E., Botchan, M.R., and Berger, J.M. (2013). A Meier-Gorlin syndrome mutation in a conserved C-terminal helix of Orc6 impedes origin recognition complex formation. eLife *2*, e00882.

Bleichert, F., Botchan, M.R., and Berger, J.M. (2015). Crystal structure of the eukaryotic origin recognition complex. Nature *519*, 321–326.

Bleichert, F., Botchan, M.R., and Berger, J.M. (2017). Mechanisms for initiating cellular DNA replication. Science *355*, eaah6317.

Bochman, M.L., and Schwacha, A. (2007). Differences in the single-stranded DNA binding activities of MCM2-7 and MCM467: MCM2 and MCM5 define a slow ATP-dependent step. J. Biol. Chem. *282*, 33795–33804.

Bochman, M.L., and Schwacha, A. (2010). The Saccharomyces cerevisiae Mcm6/2 and Mcm5/3 ATPase active sites contribute to the function of the putative Mcm2-7 'gate'. Nucleic Acids Res. *38*, 6078–6088.

Bochman, M.L., and Schwacha, A. (2015). DNA replication: strand separation unravelled. Nature *524*, 166–167.

Bowers, J.L., Randell, J.C., Chen, S., and Bell, S.P. (2004). ATP hydrolysis by ORC catalyzes reiterative Mcm2-7 assembly at a defined origin of replication. Mol. Cell *16*, 967–978.

Bramhill, D., and Kornberg, A. (1988). Duplex opening by dnaA protein at novel sequences in initiation of replication at the origin of the E. coli chromosome. Cell *52*, 743–755.

Chen, S., de Vries, M.A., and Bell, S.P. (2007). Orc6 is required for dynamic recruitment of Cdt1 during repeated Mcm2-7 loading. Genes Dev. *21*, 2897–2907.

Chen, Z., Speck, C., Wendel, P., Tang, C., Stillman, B., and Li, H. (2008). The architecture of the DNA replication origin recognition complex in Saccharomyces cerevisiae. Proc. Natl. Acad. Sci. USA *105*, 10326–10331.

Chong, J.P., Hayashi, M.K., Simon, M.N., Xu, R.M., and Stillman, B. (2000). A double-hexamer archaeal minichromosome maintenance protein is an ATP-dependent DNA helicase. Proc. Natl. Acad. Sci. USA *97*, 1530–1535.

Costa, A., Ilves, I., Tamberg, N., Petojevic, T., Nogales, E., Botchan, M.R., and Berger, J.M. (2011). The structural basis for MCM2-7 helicase activation by GINS and Cdc45. Nat. Struct. Mol. Biol. *18*, 471–477.

Costa, A., Hood, I.V., and Berger, J.M. (2013). Mechanisms for initiating cellular DNA replication. Annu. Rev. Biochem. *82*, 25–54.

Coster, G., Frigola, J., Beuron, F., Morris, E.P., and Diffley, J.F. (2014). Origin licensing requires ATP binding and hydrolysis by the MCM replicative helicase. Mol. Cell *55*, 666–677.

Deegan, T.D., and Diffley, J.F. (2016). MCM: one ring to rule them all. Curr. Opin. Struct. Biol. *37*, 145–151.

Deegan, T.D., Yeeles, J.T., and Diffley, J.F. (2016). Phosphopeptide binding by Sld3 links Dbf4-dependent kinase to MCM replicative helicase activation. EMBO J. *35*, 961–973.

Devbhandari, S., Jiang, J., Kumar, C., Whitehouse, I., and Remus, D. (2017). Chromatin constrains the initiation and elongation of DNA replication. Mol. Cell *65*, 131–141.

Duderstadt, K.E., Chuang, K., and Berger, J.M. (2011). DNA stretching by bacterial initiators promotes replication origin opening. Nature *478*, 209–213.

Duzdevich, D., Warner, M.D., Ticau, S., Ivica, N.A., Bell, S.P., and Greene, E.C. (2015). The dynamics of eukaryotic replication initiation: origin specificity, licensing, and firing at the single-molecule level. Mol. Cell *58*, 483–494.

Evrin, C., Clarke, P., Zech, J., Lurz, R., Sun, J., Uhle, S., Li, H., Stillman, B., and Speck, C. (2009). A double-hexameric MCM2-7 complex is loaded onto origin DNA during licensing of eukaryotic DNA replication. Proc. Natl. Acad. Sci. USA *106*, 20240–20245.

Fernández-Cid, A., Riera, A., Tognetti, S., Herrera, M.C., Samel, S., Evrin, C., Winkler, C., Gardenal, E., Uhle, S., and Speck, C. (2013). An ORC/Cdc6/MCM2-7 complex is formed in a multistep reaction to serve as a platform for MCM double-hexamer assembly. Mol. Cell *50*, 577–588.

Fletcher, R.J., Bishop, B.E., Leon, R.P., Sclafani, R.A., Ogata, C.M., and Chen, X.S. (2003). The structure and function of MCM from archaeal M. thermoautotrophicum. Nat. Struct. Biol. *10*, 160–167.

Fletcher, R.J., Shen, J., Gómez-Llorente, Y., Martín, C.S., Carazo, J.M., and Chen, X.S. (2005). Double hexamer disruption and biochemical activities of Methanobacterium thermoautotrophicum MCM. J. Biol. Chem. *280*, 42405–42410.

Foltman, M., Evrin, C., De Piccoli, G., Jones, R.C., Edmondson, R.D., Katou, Y., Nakato, R., Shirahige, K., and Labib, K. (2013). Eukaryotic replisome components cooperate to process histones during chromosome replication. Cell Rep. *3*, 892–904.

Frigola, J., Remus, D., Mehanna, A., and Diffley, J.F. (2013). ATPase-dependent quality control of DNA replication origin licensing. Nature *495*, 339–343.

Gibson, S.I., Surosky, R.T., and Tye, B.K. (1990). The phenotype of the minichromosome maintenance mutant mcm3 is characteristic of mutants defective in DNA replication. Mol. Cell. Biol. *10*, 5707–5720.

Gille, H., and Messer, W. (1991). Localized DNA melting and structural perturbations in the origin of replication, oriC, of Escherichia coli in vitro and in vivo. EMBO J. *10*, 1579–1584.

Gros, J., Kumar, C., Lynch, G., Yadav, T., Whitehouse, I., and Remus, D. (2015). Post-licensing specification of eukaryotic replication origins by facilitated Mcm2-7 sliding along DNA. Mol. Cell *60*, 797–807.

Heller, R.C., Kang, S., Lam, W.M., Chen, S., Chan, C.S., and Bell, S.P. (2011). Eukaryotic origin-dependent DNA replication in vitro reveals sequential action of DDK and S-CDK kinases. Cell *146*, 80–91.

Hesketh, E.L., Parker-Manuel, R.P., Chaban, Y., Satti, R., Coverley, D., Orlova, E.V., and Chong, J.P. (2015). DNA induces conformational changes in a

recombinant human minichromosome maintenance complex. J. Biol. Chem. *290*, 7973–7979.

Holthoff, H.P., Hameister, H., and Knippers, R. (1996). A novel human Mcm protein: homology to the yeast replication protein Mis5 and chromosomal location. Genomics *37*, 131–134.

Huang, H., Strømme, C.B., Saredi, G., Hödl, M., Strandsby, A., González-Aguilera, C., Chen, S., Groth, A., and Patel, D.J. (2015). A unique binding mode enables MCM2 to chaperone histones H3-H4 at replication forks. Nat. Struct. Mol. Biol. *22*, 618–626.

Jacob, F., Brenner, S., and Cuzin, F. (1964). On the regulation of DNA replication in bacteria. Cold Spring Harb. Symp. Quant. Biol. *28*, 329–348.

Kang, S., Warner, M.D., and Bell, S.P. (2014). Multiple functions for Mcm2-7 ATPase motifs during replication initiation. Mol. Cell *55*, 655–665.

Kubota, Y., Mimura, S., Nishimoto, S., Masuda, T., Nojima, H., and Takisawa, H. (1997). Licensing of DNA replication by a multi-protein complex of MCM/P1 proteins in Xenopus eggs. EMBO J. *16*, 3320–3331.

Kurat, C.F., Yeeles, J.T., Patel, H., Early, A., and Diffley, J.F. (2017). Chromatin controls DNA replication origin selection, lagging-strand synthesis, and replication fork rates. Mol. Cell *65*, 117–130.

Labib, K., Tercero, J.A., and Diffley, J.F. (2000). Uninterrupted MCM2-7 function required for DNA replication fork progression. Science *288*, 1643–1647.

Lei, M., Kawasaki, Y., Young, M.R., Kihara, M., Sugino, A., and Tye, B.K. (1997). Mcm2 is a target of regulation by Cdc7-Dbf4 during the initiation of DNA synthesis. Genes Dev. *11*, 3365–3374.

Levitt, M. (1983). Protein folding by restrained energy minimization and molecular dynamics. J. Mol. Biol. *170*, 723–764.

Levitt, M., Hirshberg, M., Sharon, R., and Daggett, V. (1995). Potential energy function and parameters for simulations of the molecular dynamics of proteins and nucleic acids in solution. Comput. Phys. Commun. *91*, 215–231.

Li, N., Zhai, Y., Zhang, Y., Li, W., Yang, M., Lei, J., Tye, B.K., and Gao, N. (2015). Structure of the eukaryotic MCM complex at 3.8 Å. Nature *524*, 186–191.

Liu, C., Wu, R., Zhou, B., Wang, J., Wei, Z., Tye, B.K., Liang, C., and Zhu, G. (2012). Structural insights into the Cdt1-mediated MCM2-7 chromatin loading. Nucleic Acids Res. *40*, 3208–3217.

Maine, G.T., Sinha, P., and Tye, B.K. (1984). Mutants of S. cerevisiae defective in the maintenance of minichromosomes. Genetics *106*, 365–385.

Maric, M., Maculins, T., De Piccoli, G., and Labib, K. (2014). Cdc48 and a ubiquitin ligase drive disassembly of the CMG helicase at the end of DNA replication. Science *346*, 1253596.

Martinez, M.P., Wacker, A.L., Bruck, I., and Kaplan, D.L. (2017). Eukaryotic replicative helicase subunit interaction with DNA and its role in DNA replication. Genes (Basel) *8*, E117.

Miller, J.M., and Enemark, E.J. (2015). Archaeal MCM proteins as an analog for the eukaryotic Mcm2-7 helicase to reveal essential features of structure and function. Archaea *2015*, 305497.

Mizushima, T., Takahashi, N., and Stillman, B. (2000). Cdc6p modulates the structure and DNA binding activity of the origin recognition complex in vitro. Genes Dev. *14*, 1631–1641.

Moir, D., Stewart, S.E., Osmond, B.C., and Botstein, D. (1982). Cold-sensitive cell-division-cycle mutants of yeast: isolation, properties, and pseudoreversion studies. Genetics *100*, 547–563.

Parker, M.W., Botchan, M.R., and Berger, J.M. (2017). Mechanisms and regulation of DNA replication initiation in eukaryotes. Crit. Rev. Biochem. Mol. Biol. *52*, 107–144.

Ramer, M.D., Suman, E.S., Richter, H., Stanger, K., Spranger, M., Bieberstein, N., and Duncker, B.P. (2013). Dbf4 and Cdc7 proteins promote DNA replication through interactions with distinct Mcm2-7 protein subunits. J. Biol. Chem. *288*, 14926–14935.

Remus, D., Beuron, F., Tolun, G., Griffith, J.D., Morris, E.P., and Diffley, J.F. (2009). Concerted loading of Mcm2-7 double hexamers around DNA during DNA replication origin licensing. Cell *139*, 719–730.

Richardson, T.T., Harran, O., and Murray, H. (2016). The bacterial DnaA-trio replication origin element specifies single-stranded DNA initiator binding. Nature *534*, 412–416.

Richet, N., Liu, D., Legrand, P., Velours, C., Corpet, A., Gaubert, A., Bakail, M., Moal-Raisin, G., Guerois, R., Compper, C., et al. (2015). Structural insight into how the human helicase subunit MCM2 may act as a histone chaperone together with ASF1 at the replication fork. Nucleic Acids Res. *43*, 1905–1917.

Riera, A., Tognetti, S., and Speck, C. (2014). Helicase loading: how to build a MCM2-7 double-hexamer. Semin. Cell Dev. Biol. *30*, 104–109.

Rother, M., Rother, K., Puton, T., and Bujnicki, J.M. (2011). ModeRNA: a tool for comparative modeling of RNA 3D structure. Nucleic Acids Res. *39*, 4007–4022.

Rowley, A., Cocker, J.H., Harwood, J., and Diffley, J.F. (1995). Initiation complex assembly at budding yeast replication origins begins with the recognition of a bipartite sequence by limiting amounts of the initiator, ORC. EMBO J. *14*, 2631–2641.

Samson, R.Y., and Bell, S.D. (2013). MCM loading—an open-and-shut case? Mol. Cell *50*, 457–458.

Samson, R.Y., and Bell, S.D. (2016). Chapter Five: archaeal DNA replication origins and recruitment of the MCM replicative helicase. In The Enzymes, S.K. Laurie and O. Marcos Túlio, eds. (Academic Press), pp. 169–190.

Sheu, Y.J., Kinney, J.B., Lengronne, A., Pasero, P., and Stillman, B. (2014). Domain within the helicase subunit Mcm4 integrates multiple kinase signals to control DNA replication initiation and fork progression. Proc. Natl. Acad. Sci. USA *111*, E1899–E1908.

Slaymaker, I.M., and Chen, X.S. (2012). MCM structure and mechanics: what we have learned from archaeal MCM. In The Eukaryotic Replisome: a Guide to Protein Structure and Function, S. MacNeill, ed. (Springer Netherlands), pp. 89–111.

Speck, C., and Messer, W. (2001). Mechanism of origin unwinding: sequential binding of DnaA to double- and single-stranded DNA. EMBO J. *20*, 1469–1476.

Speck, C., and Stillman, B. (2007). Cdc6 ATPase activity regulates ORC x Cdc6 stability and the selection of specific DNA sequences as origins of DNA replication. J. Biol. Chem. *282*, 11705–11714.

Speck, C., Chen, Z., Li, H., and Stillman, B. (2005). ATPase-dependent cooperative binding of ORC and Cdc6 to origin DNA. Nat. Struct. Mol. Biol. *12*, 965–971.

Sun, J., Kawakami, H., Zech, J., Speck, C., Stillman, B., and Li, H. (2012). Cdc6-induced conformational changes in ORC bound to origin DNA revealed by cryo-electron microscopy. Structure *20*, 534–544.

Sun, J., Evrin, C., Samel, S.A., Fernández-Cid, A., Riera, A., Kawakami, H., Stillman, B., Speck, C., and Li, H. (2013). Cryo-EM structure of a helicase loading intermediate containing ORC-Cdc6-Cdt1-MCM2-7 bound to DNA. Nat. Struct. Mol. Biol. *20*, 944–951.

Sun, J., Fernandez-Cid, A., Riera, A., Tognetti, S., Yuan, Z., Stillman, B., Speck, C., and Li, H. (2014). Structural and mechanistic insights into Mcm2-7 double-hexamer assembly and function. Genes Dev. *28*, 2291–2303.

Ticau, S., Friedman, L.J., Ivica, N.A., Gelles, J., and Bell, S.P. (2015). Single-molecule studies of origin licensing reveal mechanisms ensuring bidirectional helicase loading. Cell *161*, 513–525.

Ticau, S., Friedman, L.J., Champasa, K., Corrêa, I.R., Jr., Gelles, J., and Bell, S.P. (2017). Mechanism and timing of Mcm2-7 ring closure during DNA replication origin licensing. Nat. Struct. Mol. Biol. *24*, 309–315.

Tocilj, A., On, K.F., Yuan, Z., Sun, J., Elkayam, E., Li, H., Stillman, B., and Joshua-Tor, L. (2017). Structure of the active form of human origin recognition complex and its ATPase motor module. eLife *6*, e20818.

Wang, H., Wang, M., Yang, N., and Xu, R.M. (2015). Structure of the quaternary complex of histone H3-H4 heterodimer with chaperone ASF1 and the replicative helicase subunit MCM2. Protein Cell *6*, 693–697.

Wu, R., Wang, J., and Liang, C. (2012). Cdt1p, through its interaction with Mcm6p, is required for the formation, nuclear accumulation and chromatin loading of the MCM complex. J. Cell Sci. *125*, 209–219.

Yan, H., Gibson, S., and Tye, B.K. (1991). Mcm2 and Mcm3, two proteins important for ARS activity, are related in structure and function. Genes Dev. *5*, 944–957.

Yanagi, K., Mizuno, T., You, Z., and Hanaoka, F. (2002). Mouse geminin inhibits not only Cdt1-MCM6 interactions but also a novel intrinsic Cdt1 DNA binding activity. J. Biol. Chem. *277*, 40871–40880.

Yardimci, H., and Walter, J.C. (2014). Prereplication-complex formation: a molecular double take? Nat. Struct. Mol. Biol. *21*, 20–25.

Yeeles, J.T., Janska, A., Early, A., and Diffley, J.F. (2017). How the eukaryotic replisome achieves rapid and efficient DNA replication. Mol. Cell *65*, 105–116.

Yuan, Z., Riera, A., Bai, L., Sun, J., Nandi, S., Spanos, C., Chen, Z.A., Barbon, M., Rappsilber, J., Stillman, B., et al. (2017). Structural basis of Mcm2-7 replicative helicase loading by ORC-Cdc6 and Cdt1. Nat. Struct. Mol. Biol. *24*, 316–324.

Zhai, Y., Cheng, E., Wu, H., Li, N., Yung, P.Y., Gao, N., and Tye, B.K. (2017). Open-ringed structure of the Cdt1-Mcm2-7 complex as a precursor of the MCM double hexamer. Nat. Struct. Mol. Biol. *24*, 300–308.

Zhang, J., Yu, L., Wu, X., Zou, L., Sou, K.K., Wei, Z., Cheng, X., Zhu, G., and Liang, C. (2010). The interacting domains of hCdt1 and hMcm6 involved in the chromatin loading of the MCM complex in human cells. Cell Cycle *9*, 4848–4857.